RESEARCH ARTICLE

Involvement of FtsE ATPase and FtsX Extracellular Loops 1 and 2 in FtsEX-PcsB Complex Function in Cell Division of *Streptococcus pneumoniae* D39

Lok-To Sham, Katelyn R. Jensen, Kevin E. Bruce, Malcolm E. Winkler

Department of Biology, Indiana University Bloomington, Bloomington, Indiana, USA

L.-T.S. and K.R.J. contributed equally to this work.

Dedicated to the memory of Amy L. Davidson (Purdue University).

ABSTRACT **The FtsEX protein complex has recently been proposed to play a major role in coordinating peptidoglycan (PG) remodeling by hydrolases with the division of bacterial cells. According to this model, cytoplasmic FtsE ATPase interacts with the FtsZ divisome and FtsX integral membrane protein and powers allosteric activation of an extracellular hydrolase interacting with FtsX. In the major human respiratory pathogen *Streptococcus pneumoniae* (pneumococcus), a large extracellular-loop domain of FtsX (ECL1^{FtsX}) is thought to interact with the coiled-coil domain of the PcsB protein, which likely functions as a PG amidase or endopeptidase required for normal cell division. This paper provides evidence for two key tenets of this model. First, we show that FtsE protein is essential, that depletion of FtsE phenocopies cell defects caused by depletion of FtsX or PcsB, and that changes of conserved amino acids in the FtsE ATPase active site are not tolerated. Second, we show that temperature-sensitive (Ts) *pcsB* mutations resulting in amino acid changes in the PcsB coiled-coil domain (CC^{PcsB}) are suppressed by *ftsX* mutations resulting in amino acid changes in the distal part of ECL1^{FtsX} or in a second, small extracellular-loop domain (ECL2^{FtsX}). Some FtsX suppressors are allele specific for changes in CC^{PcsB}, and no FtsX suppressors were found for amino acid changes in the catalytic PcsB CHAP domain (CHAP^{PcsB}). These results strongly support roles for both ECL1^{FtsX} and ECL2^{FtsX} in signal transduction to the coiled-coil domain of PcsB. Finally, we found that *pcsB*^{CC}(Ts) mutants (Ts mutants carrying mutations in the region of *pcsB* corresponding to the coiled-coil domain) unexpectedly exhibit delayed stationary-phase autolysis at a permissive growth temperature.**

IMPORTANCE **Little is known about how FtsX interacts with cognate PG hydrolases in any bacterium, besides that ECL1^{FtsX} domains somehow interact with coiled-coil domains. This work used powerful genetic approaches to implicate a specific region of pneumococcal ECL1^{FtsX} and the small ECL2^{FtsX} in the interaction with CC^{PcsB}. These findings identify amino acids important for *in vivo* signal transduction between FtsX and PcsB for the first time. This paper also supports the central hypothesis that signal transduction between pneumococcal FtsX and PcsB is linked to ATP hydrolysis by essential FtsE, which couples PG hydrolysis to cell division. The classical genetic approaches used here can be applied to dissect interactions of other integral membrane proteins involved in PG biosynthesis. Finally, delayed autolysis of the *pcsB*^{CC}(Ts) mutants suggests that the FtsEX-PcsB PG hydrolase may generate a signal in the PG necessary for activation of the major LytA autolysin as pneumococcal cells enter stationary phase.**

Received 8 June 2013 **Accepted** 18 June 2013 **Published** 16 July 2013

Citation Sham L-T, Jensen KR, Bruce KE, Winkler ME. 2013. Involvement of FtsE ATPase and FtsX extracellular loops 1 and 2 in FtsEX-PcsB complex function in cell division of *Streptococcus pneumoniae* D39. mBio 4(4):e00431-13. doi:10.1128/mBio.00431-13.

Editor Stanley Maloy, San Diego State University

Address correspondence to Malcolm E. Winkler, winklerm@indiana.edu.

Peptidoglycan (PG) biosynthesis requires the regulated activities of the synthetic penicillin-binding proteins, numerous modification enzymes, and PG hydrolases (reviewed in references 1 to 3). PG hydrolases are required to cleave various bonds in mature PG and thereby allow access points for insertion of newly synthesized glycan strands (4–6). They also allow the ultimate separation of daughter cells (7, 8). The roles of PG hydrolases in PG remodeling during cell division are only starting to be understood, partly because most bacterial species contain functionally redundant division PG hydrolases, and PG hydrolases play roles in processes other than division, including PG recycling, programmed lysis during sporulation, bacterial predation, resuscitation following dormancy, and fratricide during competence (7, 9–11).

The activities of division PG hydrolases have to be carefully regulated to coordinate PG cleavage with stage of cell division and to prevent PG damage that could be catastrophic (2, 5, 7). An emerging model is that division PG hydrolases are intrinsically inactive due to limited access to their active sites or to autoinhibitory α-helices that block active sites (5, 12, 13). Inhibition is re-

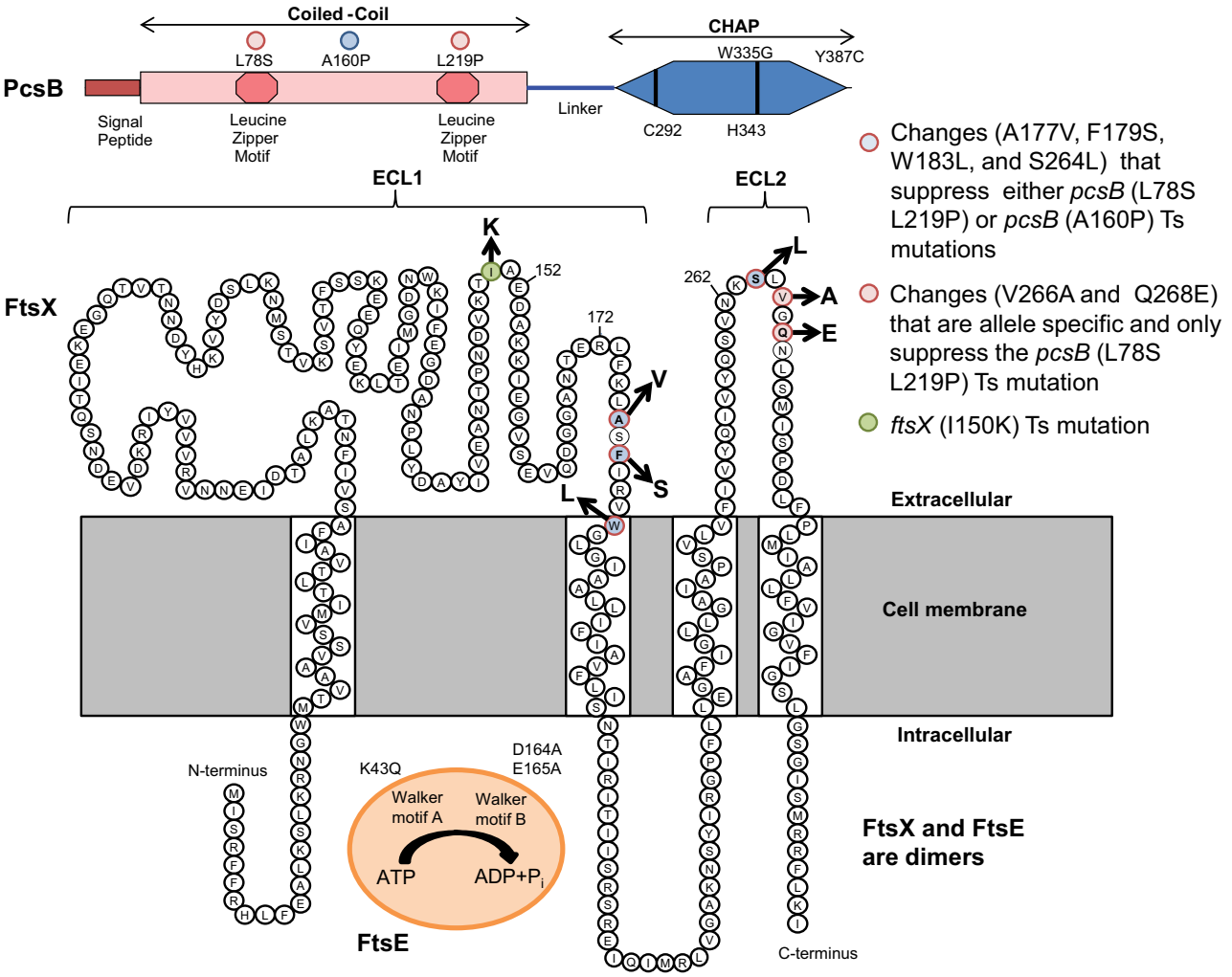

FIG 1 Summary of PcsB, FtsX, and FtsE domains and amino acid changes described in this paper. (Top) PcsB. Locations of changes in PcsB$^{L78S\text{-}L219P}$(Ts) (red dots) and PcsB^{A160P}(Ts) (blue dot) in CC^{PcsB} and PcsB^{W335G}(Ts) and PcsB^{Y387C}(Ts) in CHAP^{PcsB} are indicated. Other structural features include the signal peptide, which is processed from the mature protein, the leucine zipper motifs in CC^{PcsB}, and the required active-site amino acids Cys292 and His343 in CHAP^{PcsB} (24). (Middle) FtsX. The predicted topology of FtsX is based on reference 19. Amino acid changes that suppress *pcsB*(Ts) mutations are color coded as indicated. The FtsX^{I150K} change is also indicated. (Bottom) FtsE. The K43Q mutation and the D164A and E165A mutations in the Walker A and B motifs, respectively, are indicated. See the text for additional details.

lieved by allosteric interactions with regulatory proteins that couple PG hydrolysis to stages of cell division (5, 12, 13). The conserved FtsEX complex recently emerged as a major regulator of PG hydrolysis during bacterial cell division (2, 7, 14, 15). FtsEX is essential or conditionally essential in a variety of bacterial species (see Table S1 in the supplemental material), with the exception of low-GC Gram-positive bacilli, which may contain redundant mechanisms for FtsEX function (5, 16, 17). FtsEX structurally resembles an ABC transporter (18), although several pieces of evidence suggest that FtsEX acts as a signal transduction system, rather than as a transporter of an unknown substrate (19, 20). FtsX is an integral membrane protein with cytoplasmic amino and carboxyl termini, 4 transmembrane segments, and 1 large and 1 small extracellular loop (ECL1 and ECL2, respectively) (Fig. 1) (19). The transmembrane helices of FtsX lack charged residues that are found in canonical ABC transporters, and no putative extracellular substrate-binding protein is transcribed near *ftsEX* (19). Moreover, FtsX interacts with FtsA and FtsQ, FtsE interacts with FtsZ, and the FtsE ATPase promotes septal ring constriction in *Escherichia coli* (1, 19, 21, 22). Together, these results favor a role for FtsEX in promoting complex formation during cell division, rather than acting as a transporter.

Involvement of FtsEX as a regulator of PG hydrolysis was reported concurrently in *E. coli* and *Streptococcus pneumoniae* (14, 15). In *E. coli*, FtsEX is conditionally essential and required for growth in media with low osmotic strength (15, 20). ECL1 of FtsX$_{Eco}$ interacts with a coiled-coil domain of the EnvC activator protein, which in turn activates PG amidases AmiA and AmiB, whose activity is autoinhibited (13, 15). In contrast, pneumococcal FtsEX is essential, and the ECL1 of FtsX$_{Spn}$ interacts with the coiled-coil domain in the amino terminus of the PcsB protein (CC^{PcsB}) (14) (Fig. 1). PcsB is essential for growth of serotype 2 strains of *S. pneumoniae* (23, 24), and the absence of PcsB severely impairs growth in other serotypes of *S. pneumoniae* (25; our unpublished results). Besides its coiled-coil domain, PcsB contains a carboxyl-terminal CHAP domain (CHAP^{PcsB}), found in PG ami-

dases and endopeptidases (5). Although purified PcsB lacks PG hydrolytic activity, probably due to some type of autoinhibition, changes to the catalytic cysteine (Cys) 292 and histidine (His) 343 are not tolerated (24), and amino acid changes in $CHAP^{PcsB}$ cause temperature sensitivity (Ts) (Fig. 1) (14), strongly implying that PcsB acts as a PG hydrolase. PcsB localizes to division equators and septa, and depletion of FtsX releases PcsB into the growth medium (14).

In this paper, we report the isolation of several new classes of mutations to assess the functions and interactions of the FtsEX-PcsB complex in *S. pneumoniae*. These experiments confirm the expectation that FtsE ATPase is required for pneumococcal cell division and viability. Suppressor analysis implicates both ECL1 and ECL2 of FtsX in interactions with CC^{PcsB} and provides strong support for signal transduction between the FtsEX complex and PcsB. Finally, phenotypes of $pcsB^{CC}$(Ts), $ftsX^{ECL2}$(Sup), and $ftsX^{ECL1}$(Ts) mutants revealed a wider role of the FtsEX-PcsB complex in pneumococcal autolysis.

RESULTS

FtsE is essential in *S. pneumoniae* D39, and depletion of FtsE phenocopies PcsB or FtsX depletion. Previously, we demonstrated that *pcsB* and *ftsX* are both essential in *S. pneumoniae* serotype 2 strain D39 (14, 23, 24). Depletion of FtsX led to defects in cell division similar to those seen with depletion of PcsB, suggesting that PcsB and FtsX are involved in the same biological process (14). Since FtsE and FtsX directly interact in *E. coli* and *S. pneumoniae* (1, 19, 26), we expected that depletion of FtsE would phenocopy depletion of PcsB or FtsX. To minimize leaky expression of FtsE, we fused $ftsE^+$ to the P_{fcsK} fucose-inducible promoter and *fcsK* ribosome-binding site, followed by the *walJ* transcription terminator in the ectopic CEP site in the pneumococcal chromosome (strain IU5382) (see Table S2 in the supplemental material) (27). We then deleted *ftsE* from its native locus and screened for colonies that require fucose for growth. The resulting strain IU5756 (Δ*ftsE*::P-*erm* [deletion of codons 21 to 195 of 231]//CEP::P_{fcsK}-$ftsE^+$) grew similarly to parent strain IU5382 ($ftsE^+$//CEP::P_{fcsK}-$ftsE^+$) in BHI broth containing 0.8% (wt/vol) fucose (where // designates a separate chromosomal location) (Fig. 2A; data not shown). Reducing the amount of fucose to 0.05% (wt/vol) reduced the growth yield but not the growth rate of cultures. FtsE-depleted cells formed chains of compacted, semispherical cells that showed misplaced peripheral and septal labeling by fluorescent vancomycin, which labels regions of active PG synthesis (Fig. 2B) (23, 24). Upon removal of fucose, IU5756 cultures stopped growing after ~400 min and did not lyse within the additional ~200 min monitored. Cells severely depleted for FtsE became more spherical and showed aberrant placement of PG synthesis (Fig. 2B, images A8, A13, and A15). These phenotypes match those reported previously for depletion of PcsB or FtsX (14, 23, 24), consistent with FtsE, FtsX, and PcsB acting together in cell division.

Amino acid changes in the conserved Walker motifs of FtsE are not tolerated by *S. pneumoniae* D39. Conserved amino acids in the ATP binding pocket of the Walker A and Walker B motifs of FtsE were shown to be critical for FtsE function in *E. coli* (15, 19). Changes in these amino acids impaired FtsZ ring constriction during *E. coli* cell division, resulting in the formation of elongated cells, like those observed in Δ*ftsE* mutants (15, 19). We tested whether comparable amino acid changes in the ATP binding

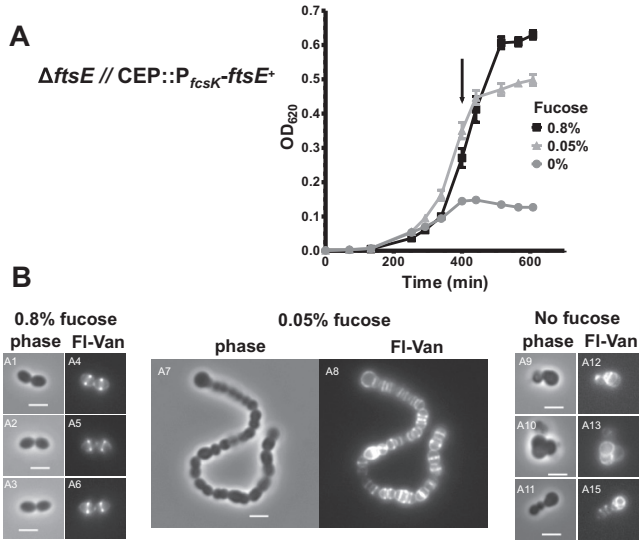

FIG 2 Depletion of FtsE phenocopies depletion of PcsB and FtsX. Cells of strain IU5756 (Δ*ftsE*::P-*erm*//CEP::P_{fcsK}-*ftsE*) were grown in BHI broth containing 0.4% fucose at 37°C, collected by centrifugation, washed once with BHI broth lacking fucose, and resuspended in BHI broth containing 0.8% (wt/vol), 0.05% (wt/vol), and 0% fucose, and growth was monitored (see Materials and Methods). (A) Representative growth curves following the shift to the concentrations of L-fucose indicated. (B) After 400 min (arrow in panel A), cells were collected, stained with fluorescent vancomycin (Fl-Van), and visualized by microscopy (see Materials and Methods). Bar, 2 μm. Replicate independent experiments were done more than 3 times with similar results.

pocket of pneumococcal FtsE resulted in a lethal phenotype (Fig. 1). Mutant alleles *ftsE* (K43A), *ftsE* (D164A), and *ftsE* (E165A) were exchanged into the *ftsE* chromosomal locus in a merodiploid strain that expresses $ftsE^+$ from the ectopic CEP site (strain IU5818 [Δ*ftsE*::P-*kan* $rpsL^+$//CEP::P_{fcsK}-$ftsE^+$]) (see Materials and Methods; also, see Table S2 in the supplemental material). The resulting strains (IU6023, IU6025, and IU6027) required 0.8% (wt/vol) fucose for growth and formation of wild-type-looking cells (Fig. 3; also, see Fig. S1 in the supplemental material).

Removal of fucose and depletion of $FtsE^+$ led to growth cessation and formation of spherical cells with aberrant division planes, similar to those observed when ectopically expressed $FtsE^+$ was depleted in a Δ*ftsE* mutant (Fig. 2). Interestingly, the *ftsE* (K43A, D164A, and E165A)//CEP::P_{fcsK}-$ftsE^+$ mutants showed significantly reduced growth in low (0.05% [wt/vol]) fucose (Fig. 3A), whereas in repeated independent experiments, the Δ*ftsE*//CEP::P_{fcsK}-$ftsE^+$ mutant grew normally until cultures possibly ran out of fucose (Fig. 2A). Although we do not know the level of FtsE expressed from the ectopic CEP site in 0.05% (wt/vol) fucose, the impaired growth of the *ftsE* (K43A, D164A, and E165A)//CEP::P_{fcsK}-$ftsE^+$ mutants is consistent with a dominant negative effect of the mutant FtsE in dimers with wild-type FtsE. From these combined results, we conclude that FtsE ATPase is required for pneumococcal cell division.

Isolation of *ftsX* mutations that suppress $pcsB^{CC}$(Ts) mutations. Previously, we reported that Ts mutations can be isolated in $pcsB^{CC}$ and $pcsB^{CHAP}$, indicating the requirement of these two domains for PcsB function in pneumococcal cells (14). Four *pcsB*(Ts) mutations were used in this study. $pcsB^{L78S\text{-}L219P}$ changes two leucines in the tandem zipper motifs of CC^{PcsB}, and both

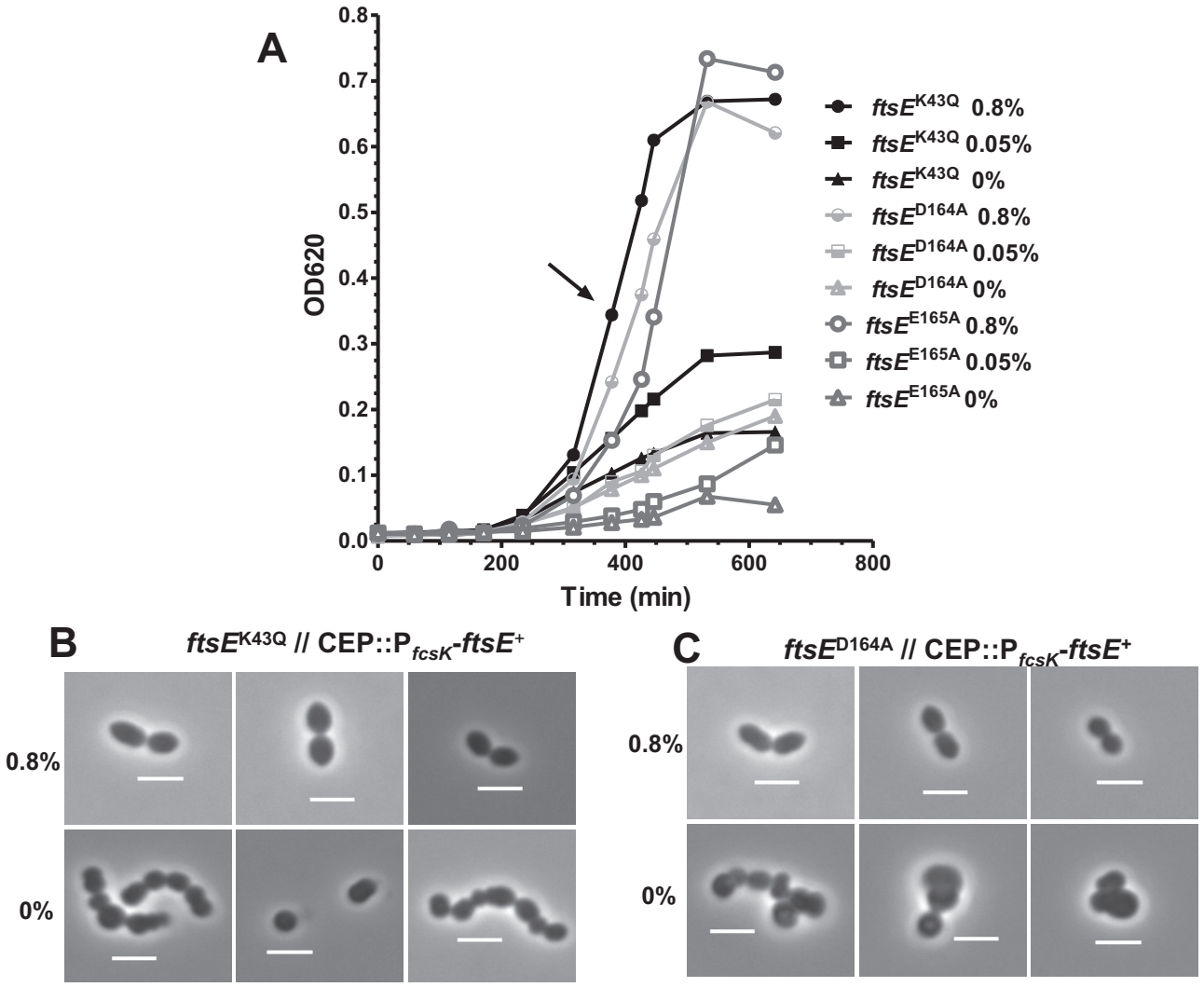

FIG 3 Amino acid changes FtsE^{K43Q}, FtsE^{D164A}, and FtsE^{E165A} in the Walker A and B motifs of FtsE are not tolerated. Strain IU6023 (IU1824 *ftsE*^{K43Q}//CEP::P$_{fcsK}$-*ftsE*$^{+}$), IU6025 (IU1824 *ftsE*^{D164A}//CEP::P$_{fcsK}$-*ftsE*$^{+}$), and IU6027 (IU1824 *ftsE*^{E165A}//CEP::P$_{fcsK}$-*ftsE*$^{+}$) were grown in BHI broth supplemented with 0.4% (wt/vol) fucose overnight. Cells were collected by centrifugation, washed with BHI broth lacking fucose, and resuspend to an OD_{620} of ~0.001 in BHI broth containing 0.8% (wt/vol), 0.05% (wt/vol), or 0% fucose (see Materials and Methods). (A) Representative growth curves following the shift to the concentrations of L-fucose indicated. (B and C) After ~400 min (arrow in panel A), cells were observed by phase-contrast microscopy. Bar, 2 μm. Cells of strain IU6025 (C) and IU6027 (not shown) looked alike. The experiment was done twice with similar results.

changes are required to impart temperature sensitivity (Fig. 1) (14). *pcsB*^{A160P} changes an alanine, which modeling indicates may be in a hairpin region formed by interactions between the leucine zipper motifs. *pcsB*^{W335G} and *pcsB*^{Y387C} change amino acids near the active-site His343 and at the very end of CHAP^{PcsB}, respectively (Fig. 1). Previously, Western blotting showed that the cellular amount of PcsB$^{L78S\text{-}L219P}$ did not decrease at the nonpermissive (41.4°C) compared to the permissive (32°C) temperature (14). A substantial fraction (>50%) of wild-type PcsB^{+} is normally released from pneumococcal cells into broth cultures (see Fig. S2 in the supplemental material) (23), but a greater proportion of PcsB$^{L78S\text{-}L219P}$ was not released at 41.4°C than at 32°C (14). Likewise, Western blots of PcsB^{A160P}, PcsB^{W335G}, and PcsB^{Y387C} using anti-PcsB antibody showed that these mutant proteins were not destabilized or released more at 41.4°C than at 32°C (see Fig. S2), despite more overall instability of PcsB^{Y387C}, and to a lesser extent PcsB^{W335G}, than PcsB^{A160P} or PcsB^{+} at either temperature. Together, these results suggest that the PcsB(Ts) mutant proteins have lost critical signaling or catalytic functions at the nonpermissive temperature.

To gain information about the signaling between PcsB and FtsX, we used error-prone PCR to target random mutations to an amplicon containing *ftsX* linked to a downstream kanamycin resistance marker (IU4325) (see Tables S2 and S3 in the supplemental material), transformed the mutated *ftsX* amplicon into each *pcsB*(Ts) mutant, and selected for growth at the nonpermissive temperature of 41.4°C (see Materials and Methods). Screening of ~38,000 transformants of the *pcsB*$^{L78S\text{-}L219P}$(Ts) and *pcsB*^{A160P}(Ts) mutants revealed 7 different *ftsX* suppressor mutations (Table 1; also, see Table S4 in the supplemental material) that were confirmed by DNA sequencing of the chromosome region corresponding to the entire PCR amplicon used in transformations.

TABLE 1 Temperature-sensitive mutants and suppressors isolated in this study

Temperature-sensitive allele(s) (strain[s])	Corresponding suppressor allele (strain)[a]	Comment(s)
pcsB$^{L78S-L219P}$ (IU4261)	*ftsX*^{V266A} (IU6363)	Allele specific
	ftsX^{Q268E} (IU5690)	Allele specific
	ftsX$^{K88M-R204H}$ (IU6367)	Allele specific
pcsB$^{L78S-L219P}$ (IU4261) and *pcsB*^{A160P} (IU4256 and IU4262)	*ftsX*^{A177V} (IU5692; IU6525)	Not allele specific
	ftsX^{F179S} (IU6365; IU5961)	Not allele specific
	ftsX^{W183L} (IU6335; IU6333)	Not allele specific
	ftsX^{S264L} (IU6361; IU6270)	Not allele specific
pcsB^{W335G} (IU4081)	None isolated yet	See Table S4
pcsB^{Y387C} (IU4257)	None isolated	Leaky at 41.4°C; see Table S4
ftsX^{I150K} (IU6001)	In progress	See the text
ftsX$^{Y254C-I300T}$ (IU5694)	In progress	See the text

[a] *ftsX*^{F179S} and *ftsX*^{S264L} were originally isolated as suppressors of the *pcsB*^{A160P} mutation. Other *ftsX* suppressor mutations were isolated during screens of a *pcsB*$^{L78S-L219P}$ mutant. Strains are indicated from backcrosses (Table S2). *ftsX*^{A177V} was also isolated in strains IU6351, IU6385, and IU6387 with the mutations *ftsX*$^{I192V-D276Q}$ (see Table S2 in the supplemental material).

Backcrossing the *ftsX* suppressor mutations into the *pcsB*(Ts) mutant in which they were originally selected confirmed that the suppression was due solely to the *ftsX* mutations and not to mutations outside *ftsX*. In contrast to the *pcsB*^{CC}(Ts) mutations, no suppressor of the *pcsB*^{W335G}(Ts) mutation in CHAP^{PcsB} was obtained upon screening of ~16,800 colonies (Fig. 1 and Table 1; also, see Table S4 in the supplemental material), although we cannot rule out the possibility that we missed a rare suppressor mutation. The *pcsB*^{Y387C}(Ts) mutation is leaky and allows slow growth at 41.4°C, and limited screening of ~3,800 colonies did not turn up any *ftsX* suppressors of the *pcsB*^{Y387C} mutation (Table 1; also, see Table S4 in the supplemental material).

Region specificity and allele specificity of *ftsX*^{ECL1} and *ftsX*^{ECL2} suppressors of *pcsB*^{CC}(Ts) mutations. Of the seven *ftsX* suppressors of *pcsB*^{CC}(Ts) mutations isolated in this study, six resulted in single-amino-acid changes in ECL1^{FtsX} or ECL2^{FtsX} (Fig. 1). Of these six *ftsX* suppressors, three (*ftsX*^{A177V}, *ftsX*^{F179S}, and *ftsX*^{W183L}) are in the far-distal region of ECL1^{FtsX} and three (*ftsX*^{S264L}, *ftsX*^{V266A}, and *ftsX*^{Q268E}) are in the small domain ECL2^{FtsX}, which has not been characterized before (Fig. 1; Table 1). All six *ftsX* single suppressors did not suppress the *pcsB*^{W335G}(Ts) mutation in CHAP^{PcsB}, indicating that the *ftsX* suppressor mutations do not cause a general gain of function of FtsX.

We next tested the *ftsX* suppressors for allele specificity (28). The three *ftsX* mutations in ECL1^{FtsX} (*ftsX*^{A177V}, *ftsX*^{F179S}, and *ftsX*^{W183L}) and one in ECL2 (*ftsX*^{S264L}) suppressed both the *pcsB*$^{L78S-L219P}$(Ts) and *pcsB*^{A160P}(Ts) mutations, whereas two *ftsX* mutations in ECL2^{FtsX} (*ftsX*^{V266A} and *ftsX*^{Q268E}) were allele specific and suppressed only the *pcsB*$^{L78S-L219P}$(Ts) mutations. Finally, one other *ftsX* suppressor isolated in this study contained two mutations (*ftsX*$^{K88M-R204H}$), which change amino acids in the proximal region of ECL1 and in the cytoplasmic domain between ECL1 and ECL2 (Table 1). The *ftsX*$^{K88M-R204H}$ suppressor was also allele specific for the *pcsB*$^{L78S-L219P}$(Ts) mutations, but the *ftsX*$^{K88M-R204H}$ mutations were not separated or characterized further in this study. We conclude that region-specific and allele-specific suppressors clustered in the distal ECL1^{FtsX} and in ECL2^{FtsX} can correct conformational defects in the CC^{PcsB} but not in CHAP^{PcsB}.

***pcsB*$^{L78S-L219P}$(Ts), *pcsB*^{A160P}(Ts), and *ftsX*^{V266A}(Sup) mutations delay autolysis in stationary phase.** We characterized the growth of the Ts and suppressor strains described above at the permissive temperatures of 32°C and 37°C (Fig. 4A; also, see Fig. S3 in the supplemental material). The single mutants containing *pcsB*$^{L78S-L219P}$(Ts), *pcsB*^{A160P}(Ts), *ftsX*^{S264L}(Sup), or *ftsX*^{V266A}(Sup) (where Sup indicates that the mutation acts as a suppressor) and the suppressed double mutants containing *pcsB*$^{L78S-L219P}$ *ftsX*^{S264L} or *pcsB*$^{L78S-L219P}$ *ftsX*^{V266A} grew like the parent strain at 32°C (Fig. 4A; also, see Fig. S3). In contrast, the *pcsB*^{W335G}(Ts) mutant grew more slowly and to a lower yield than the other strains, even at 32°C (see Fig. S3). At 37°C, cultures of the parent strain and the single mutants containing *ftsX*^{S264L}(Sup) or *pcsB*^{W335G}(Ts) showed the characteristic drop in optical density at 620 nm (OD_{620}) in stationary phase, indicative of autolysis (Fig. 4A; also, see Fig. S3). Unexpectedly, cultures of the single mutants containing *pcsB*$^{L78S-L219P}$(Ts), *pcsB*^{A160P}(Ts), or *ftsX*^{V266A}(Sup) and the suppressed double mutants containing *pcsB*$^{L78S-L219P}$ *ftsX*^{S264L} or *pcsB*$^{L78S-L219P}$ *ftsX*^{V266A} did not show this pronounced drop in OD_{620} in stationary phase (Fig. 4A; also, see Fig. S3). Consistent with a reduced drop in OD_{620}, live-dead staining (Materials and Methods) showed that the *pcsB*$^{L78S-L219P}$(Ts) and *pcsB*^{A160P}(Ts) mutants retained cell viability in early stationary phase ($OD_{620} \approx 0.7$) at 37°C compared to a drop for the parent strain (Fig. 4B).

At 41.4°C, all of the *pcsB* Ts mutants failed to grow as expected (Fig. 4A; also, see Fig. S3). In contrast, the suppressed *pcsB*$^{L78S-L219P}$(Ts) *ftsX*^{V266A}(Sup) double mutant grew similarly to the parent strain, whereas the *pcsB*$^{L78S-L219P}$(Ts) *ftsX*^{S264L}(Sup) double mutant consistently gave higher growth yields than the parent at 41.4°C (Fig. 4A). Autolysis is caused by activation of a small amount of extracellular LytA amidase as pneumococcal cells enter stationary phase (29). In addition, LytA PG hydrolysis contributes to the autolysis that occurs when pneumococcus encounters penicillin G and in the fratricide response during competence (9, 29, 30). Consequently, we compared the culture densities of mutants containing *pcsB*$^{L78S-L219P}$(Ts) or *pcsB*^{A160P}(Ts) with an isogenic Δ*lytA* mutant as cells entered stationary phase or were treated with penicillin G (see Fig. S3D). For ~5 h in stationary phase, the *pcsB*$^{L78S-L219P}$(Ts), *pcsB*^{A160P}(Ts), and Δ*lytA* mutants maintained their culture densities compared to the parent strain and a *pcsB*^{W335G}(Ts) mutant (see Fig. S3). If left overnight, the *pcsB*$^{L78S-L219P}$(Ts) and *pcsB*^{A160P}(Ts) mutant cultures lysed, whereas the Δ*lytA* mutant culture maintained its density. At the concentration of penicillin G added, Δ*lytA* cultures stopped growing and did not lyse, whereas the *pcsB*$^{L78S-L219P}$(Ts) and *pcsB*^{A160P}(Ts) mutant cultures showed rapid autolysis like the par-

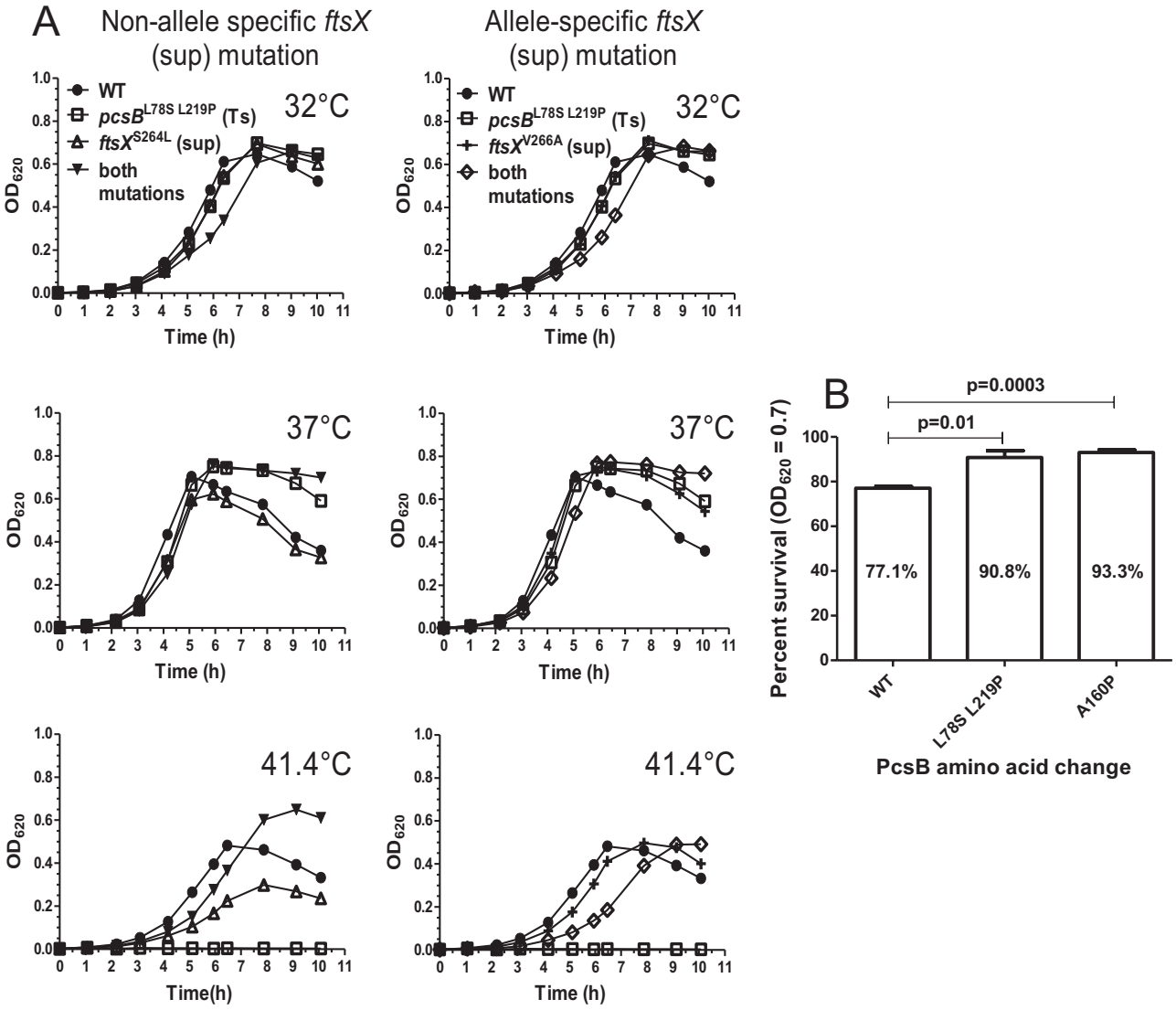

FIG 4 Delayed autolysis at 37°C of single mutants *pcsB*$^{L78S\text{-}L219P}$(Ts) and *ftsX*^{V266A}(Sup) and double *pcsB*$^{L78S\text{-}L219P}$(Ts) *ftsX*^{S264L}(Sup) and *pcsB*$^{L78S\text{-}L219P}$(Ts) *ftsX*^{V266A}(Sup) mutants. (A) Strains IU1945 (parent), IU4261 [*pcsB*$^{L78S\text{-}L219P}$(Ts)], IU6426 [*ftsX*^{S264L}(Sup)], IU6371 [*pcsB*$^{L78S\text{-}L219P}$(Ts) *ftsX*^{S264L}(Sup)], IU6439 [*ftsX*^{V266A}(Sup)], and IU6363 [*pcsB*$^{L78S\text{-}L219P}$(Ts) *ftsX*^{V266A}(Sup)] were grown in BHI broth at 32°C and diluted to an OD_{620} of ~0.001 in fresh BHI broth prewarmed to the temperatures indicated. Growth was monitored as described in Materials and Methods, and representative growth curves from more than 3 independent experiments are shown. *ftsX*^{S264L}(Sup) and *ftsX*^{V266A}(Sup) are non-allele-specific and allele-specific suppressors of *pcsB*^{CC}(Ts), respectively (Fig. 1; see the text). A comparable delay in autolysis was detected for strain IU4262 [*pcsB*^{A160P}(Ts)] (see Fig. S3 in the supplemental material). (B) At an OD_{620} of 0.7 in 37°C cultures, cells of strain IU1945 (parent), IU4261 [*pcsB*$^{L78S\text{-}L219P}$(Ts)], and IU4262 [*pcsB*^{A160P}(Ts)] were stained for viability as described in Materials and Methods. Experiments were performed independently three times ($n = 3$), and ~1,300 cells were counted per sample (B).

ent strain (see Fig. S3D). We conclude that stationary-phase autolysis is delayed, but not eliminated, by the *pcsB*$^{L78S\text{-}L219P}$(Ts) and *pcsB*^{A160P}(Ts) mutations, and these mutations do not provide any protection against the rapid autolysis induced by penicillin G treatment.

DISCUSSION

PG remodeling by hydrolases is essential for PG biosynthesis and must be carefully coordinated with specific stages of bacterial cell division (5, 6, 14, 15). In this process, endopeptidases and amidases are thought to remove cross-links between PG peptides and to cleave off PG peptides, respectively, and thereby allow insertion and cross-linking of newly synthesized glycan strands or the separation of divided cells (4–6, 31). In *S. pneumoniae*, the PcsB protein has the hallmarks of a PG hydrolase (32). Typical of many hydrolases from Gram-positive organisms, PcsB is processed and exported to the cell surface by the SecA system (23), and PcsB consists of a surface-binding domain (CC^{PcsB}) and a catalytic domain ($CHAP^{PcsB}$) (Fig. 1) (see the introduction). PcsB is a relatively abundant protein (~5,000 monomers) on the pneumococcal cell surface, yet this amount represents less than 50% of the PcsB lost to the culture medium of exponential growing *S. pneumoniae* (see Fig. S2 in the supplemental material) (14, 23). Like other regulated, remodeling PG hydrolases, purified PcsB lacking its signal peptide is catalytically inactive in a variety of assay formats, including zymograms (data not shown) (14, 23, 25). In zy-

mograms, apparent clearing by PcsB protein was not due to PG hydrolysis, because it still occurred in control experiments containing catalytically inactive PcsB Cys292Ala and His343Ala mutant proteins (data not shown). In contrast, the Cys292Ala and His343Ala amino acid changes are not tolerated in cells, consistent with an essential PG hydrolase function for PcsB (24).

The lack of PG hydrolysis activity by purified PcsB led to the hypothesis of allosteric activation of PcsB by an essential membrane protein, which was found to be FtsX in complex with FtsE (see the introduction) (Fig. 1) (2, 14, 24). In this paper, we show that FtsE, like PcsB and FtsX, is essential in serotype 2 *S. pneumoniae* (Fig. 2A), and depletion of each of these proteins leads to similar defects in cell division (Fig. 2B), consistent with a shared function. Interestingly, partial depletion of PcsB, FtsX, or FtsE causes unencapsulated pneumococcus to form chains of cells that are more spherical and compressed than those of the diplococcal parent strain (Fig. 2B) (14, 23, 24). This phenotype may indicate that decreased PG remodeling by the PcsB-FtsEX hydrolase blocks glycan chain insertion in midcell peripheral (sidewall-like) PG synthesis, which would cause formation of spherical cells (2). In addition, this paper shows that the conserved amino acids in the ATP binding site of FtsE are essential for pneumococcal growth, supporting the idea that FtsE ATPase activity is required for PcsB-FtsEX signaling and coordination with cell division. Based on the EnvC-FtsEX complex in *E. coli* (15), we expect that loss of FtsE ATPase activity will not alter the localization of the PcsB-FtsEX complex in *S. pneumoniae*. This and other hypotheses about the role of FtsE ATPase function await testing in future experiments.

This study also provides strong new support for the idea that the FtsX interaction with PcsB is mediated by interactions between ECL1^{FtsX} and ECL2^{FtsX} and CC^{PcsB}. The FtsEX complex resembles an ABC transporter (see the introduction) (18, 19), and biochemical reconstitution of FtsEX-PcsB function could be challenging (33, 34). To gain more insight into the interactions between PcsB and FtsX, we used an updated version of classical suppressor analysis (28) that combines error-prone PCR targeting of mutations with the ease of strain construction by pneumococcal transformation (see Results and Materials and Methods). We found region- and allele-specific mutations in ECL1^{FtsX} and ECL2^{FtsX} that indicate interactions between the distal portion of ECL1^{FtsX} and ECL2^{FtsX} in FtsX and CC^{PcsB}, but not CHAP^{PcsB}, in PcsB (Fig. 1 and Table 1; see Results). Alignments of ECL1 and ECL2 from different bacteria showed that the amino acid changes caused by the *ftsX* suppressor mutations are in nonconserved amino acids (see Fig. S4 in the supplemental material). This observation is consistent with the fact that ECL1 and ECL2 interact with different PG hydrolases in different bacterial species, such as PcsB in *S. pneumoniae* and EnvC-AmiA/B in *E. coli* (14, 15). Since FtsE and FtsX are likely both dimers (19, 26), our results suggest a complex interaction surface between FtsX and PcsB and indicate that biochemical interaction studies will need to include both ECL1^{FtsX} and ECL2^{FtsX}, perhaps in rigid juxtaposition. The amino acid changes identified in this study also will be invaluable in future biochemical studies.

We are currently reversing the genetic scheme described above, starting with the isolation of *ftsX*(Ts) mutants enriched by error-prone PCR. Of 10 *ftsX*(Ts) mutants isolated from several independent screens, 9 contained the single *ftsX*^{I150K} mutation, which changes a conserved isoleucine in the last third of ECL1^{FtsX} (Fig. 1 and Table 1; also, see Fig. S4 and Table S2 in the supplemental material). The remaining mutant contained two mutations: *ftsX*^{Y254C} in ECL2^{FtsX} and *ftsX*^{I300T} in the cytoplasmic domain of FtsX near its carboxyl terminus (Table 1). We are in the process of selecting for *pcsB* or *ftsE* suppressors of the *ftsX*^{I150K}(Ts) mutation. But together, these studies of FtsX show that these genetic approaches can be used to interrogate the functions and complex interactions of other integral membrane proteins involved in pneumococcal cell division.

Finally, we found that the *pcsB*$^{L78S\text{-}L219P}$(Ts), *pcsB*^{A160P}(Ts), and *ftsX*^{V266A}(Sup) mutations delay autolysis in stationary phase at 37°C (Fig. 4; also, see Fig. S3 in the supplemental material). In *S. pneumoniae*, stationary-phase autolysis is catalyzed by the LytA amidase, which is a surface choline-binding protein (9, 29). However, LytA lacks a signal export sequence, and only about 5% of cellular LytA finds its way to the surface of exponentially growing cells, where it remains inactive (29). As pneumococcal cells enter stationary phase in culture, surface LytA is thought to sense some structural signal in the PG that activates the surface LytA in some cells, thereby triggering release of cytoplasmic LytA and autolysis of the culture (29). Our results suggest that the PG signal for LytA release may be reduced by certain mutations of *pcsB* and *ftsX*, including *pcsB*$^{L78S\text{-}L219P}$(Ts), *pcsB*^{A160P}(Ts), and *ftsX*^{V266A}(Sup), thereby delaying the onset of autolysis. Previously, we showed that the PG lactoyl-peptide composition was not altered upon PcsB underexpression or depletion (23). However, recent studies have shown that depletion of some cell division PG hydrolases results in subtle changes in PG composition that require determination of PG peptides attached to glycan-chain disaccharides to be detected (4). Ongoing experiments will determine whether the PG structure of *pcsB*$^{L78S\text{-}L219P}$(Ts), *pcsB*^{A160P}(Ts), and *ftsX*^{V266A}(Sup) mutants is different from that of the isogenic *pcsB*$^{+}$ *ftsX*$^{+}$ parent strain as cells enter stationary phase.

MATERIALS AND METHODS

Bacterial strains, growth, and strain constructions. Strains used in this study (see Table S2 in the supplemental material) were constructed in an unencapsulated derivative of serotype 2 strain D39 (35), which was chosen to highlight cell morphology defects (23). Unless otherwise specified, bacteria were grown on TSAII blood agar (BA) plates or statically in Becton Dickinson brain heart infusion (BHI) broth at the temperatures indicated in the figures in an atmosphere of 5% CO_2 as described before (14, 36, 37). Overnight cultures with an OD_{620} of <0.2 were diluted in fresh BHI broth to an OD_{620} of ~0.002, and bacterial growth was monitored by determining the OD_{620} hourly as described in references 14, 36, and 37.

Strains containing site-directed point mutations, deletion mutations, or antibiotic markers were constructed by transforming linear DNA amplicons synthesized by overlapping fusion PCR into competent pneumococcal cells as described in references 23, 36, and 37. Primers synthesized and the DNA templates used for PCRs are listed in Table S3 in the supplemental material. Allele exchange of point mutations was done using the Janus cassette method as described previously (36, 38). All constructs in strains were confirmed by PCR mapping and DNA sequencing of relevant chromosomal regions as described in references 14, 36, and 37.

Depletion of FtsE^{+} in Δ*ftsE*, *ftsE*^{K43Q}, *ftsE*^{D164A}, and *ftsE*^{E165A} merodiploid strains. Procedures to deplete FtsE in pneumococcal strains IU5756 (IU1824 Δ*ftsE*::P-*erm*//CEP::P$_{fcsK}$-*ftsE*$^{+}$), IU6023 (IU1824 *ftsE*^{K43Q}//CEP::P$_{fcsK}$-*ftsE*$^{+}$), IU6025 (IU1824 *ftsE*^{D164A}//CEP::P$_{fcsK}$-*ftsE*$^{+}$), and IU6027 (IU1824 *ftsE*^{E165A}//CEP::P$_{fcsK}$-*ftsE*$^{+}$) were similar to those used to previously to deplete FtsX (14) and are described in the supplemental methods. Following washing, final cultures were inoculated to an OD_{620} of ~0.001 in 5 ml of BHI broth containing 0.8% (wt/vol), 0.05% (wt/vol), or no fucose, and growth was monitored by measuring

the OD_{620} at 37°C. Cells were observed at various times by phase-contrast microscopy and were stained with fluorescent vancomycin and observed by epifluorescent microscopy as described before (14, 23).

Determination of relative cellular amounts of the PcsB^{A160P}(Ts), PcsB^{W335G}(Ts) and PcsB^{Y387C}(Ts) proteins. Previously, we used quantitative Western blotting to show that the relative amount of the PcsB$^{L78S-L219P}$(Ts) protein and its release into the growth medium were similar at the permissive (32°C) and nonpermissive (41.4°C) temperatures and resembled the pattern detected for the wild-type PcsB^{+} protein (14). We again used quantitative Western blotting with polyclonal anti-PcsB antibody to determine the relative cellular amounts and release of the PcsB^{A160P}(Ts), PcsB^{W335G}(Ts), and PcsB^{Y387C}(Ts) proteins (see Fig. S2 and the supplemental methods in the supplemental material). Cell morphologies were observed by phase-contrast microscopy in 32°C cultures before temperature shifts ($t = 0$) and ~100 min after shifts to 41.4°C, when samples were taken for Western blotting.

Isolation of *pcsB*(Ts) suppressors in *ftsX*. A mutated "*ftsEX*^{M} P-*kan rpsL*$^{+}$" amplicon containing 0 to 4 mutations per kb was generated by error-prone PCR using primers listed in Table S3 in the supplemental material as described before (14), with the modifications described in the supplemental methods. Mutated *ftsEX*^{M} P-*kan rpsL*$^{+}$ amplicon was transformed into strains IU4261 (IU1945 *pcsB*$^{L78S-L219P}$ P_c-*erm*), IU4256 (IU1945 *pcsB*^{A160P} P_c-*erm*), IU4081 (IU1945 *pcsB*^{W335G} P_c-*erm*), and IU4262 (IU1945 *pcsB*^{Y387C} P_c-*erm*) at 32°C. Transformants were plated on BA containing 250 μg kanamycin per ml and incubated at 32°C or 41.4°C to obtain numbers of transformants or to select for suppressors of the *pcsB*(Ts) alleles, respectively. Control experiments showed that the reversion frequency of *pcsB*(Ts) mutations was negligible. Suppressor mutations in *ftsX* were confirmed by DNA sequencing and by backcrosses into the *pcsB*(Ts) mutant used for the selection, Allele specificity was determined by transformation into other *pcsB*(Ts) mutants.

Isolation of *ftsX*(Ts) mutants. Mutated *ftsEX*^{M} P-*kan rpsL*$^{+}$ amplicon was transformed into strain IU1945 (D39 Δ*cps*), and *ftsX*(Ts) mutants were screened by methods described in reference 14, with the modifications described in the supplemental methods.

Live-dead staining of *pcsB* and *ftsX* mutants in different growth phases. Live-dead staining was performed using LIVE/DEAD *Bac*Light bacterial viability kit (Molecular Probes) as described before (39) with the modifications described in the supplemental methods.

SUPPLEMENTAL MATERIAL

Supplemental material for this article may be found at http://mbio.asm.org/lookup/suppl/doi:10.1128/mBio.00431-13/-/DCSupplemental.

Text S1, DOCX file, 0.1 MB.
Figure S1, PPTX file, 0.5 MB.
Figure S2, PPT file, 2.5 MB.
Figure S3, PPTX file, 0.2 MB.
Figure S4, PDF file, 0.1 MB.
Table S1, DOCX file, 0 MB.
Table S2, DOC file, 0.2 MB.
Table S3, DOC file, 0.1 MB.
Table S4, DOC file, 0.1 MB.

ACKNOWLEDGMENTS

We thank Tiffany Tsui, Krys Kazmierczak, and David Giedroc for information, comments, and helpful discussion about this work.

This work was supported by NIAID grant AI097289 to M.E.W. and by funds from the Indiana University Bloomington METACyt Initiative, funded in part by a major grant from the Lilly Endowment, to M.E.W.

The contents of this paper are solely the responsibility of the authors and do not necessarily represent official views of the funding agencies.

REFERENCES

1. **Egan AJ, Vollmer W.** 2013. The physiology of bacterial cell division. Ann. N. Y. Acad. Sci. **1277:**8–28.
2. **Sham LT, Tsui HC, Land AD, Barendt SM, Winkler ME.** 2012. Recent advances in pneumococcal peptidoglycan biosynthesis suggest new vaccine and antimicrobial targets. Curr. Opin. Microbiol. **15:**194–203.
3. **Typas A, Banzhaf M, Gross CA, Vollmer W.** 2012. From the regulation of peptidoglycan synthesis to bacterial growth and morphology. Nat. Rev. Microbiol. **10:**123–136.
4. **Singh SK, SaiSree L, Amrutha RN, Reddy M.** 2012. Three redundant murein endopeptidases catalyse an essential cleavage step in peptidoglycan synthesis of *Escherichia coli* K12. Mol. Microbiol. **86:**1036–1051.
5. **Vollmer W.** 2012. Bacterial growth does require peptidoglycan hydrolases. Mol. Microbiol. **86:**1031–1035.
6. **Vollmer W, Joris B, Charlier P, Foster S.** 2008. Bacterial peptidoglycan (murein) hydrolases. FEMS Microbiol. Rev. **32:**259–286.
7. **Uehara T, Bernhardt TG.** 2011. More than just lysins: peptidoglycan hydrolases tailor the cell wall. Curr. Opin. Microbiol. **14:**698–703.
8. **Uehara T, Parzych KR, Dinh T, Bernhardt TG.** 2010. Daughter cell separation is controlled by cytokinetic ring-activated cell wall hydrolysis. EMBO J. **29:**1412–1422.
9. **Berg KH, Biørnstad TJ, Johnsborg O, Håvarstein LS.** 2012. Properties and biological role of streptococcal fratricins. Appl. Environ. Microbiol. **78:**3515–3522.
10. **Morlot C, Uehara T, Marquis KA, Bernhardt TG, Rudner DZ.** 2010. A highly coordinated cell wall degradation machine governs spore morphogenesis in *Bacillus subtilis*. Genes Dev. **24:**411–422.
11. **Wyckoff TJ, Taylor JA, Salama NR.** 2012. Beyond growth: novel functions for bacterial cell wall hydrolases. Trends Microbiol. **20:**540–547.
12. **Chou S, Bui NK, Russell AB, Lexa KW, Gardiner TE, LeRoux M, Vollmer W, Mougous JD.** 2012. Structure of a peptidoglycan amidase effector targeted to gram-negative bacteria by the type VI secretion system. Cell. Rep. **1:**656–664.
13. **Yang DC, Tan K, Joachimiak A, Bernhardt TG.** 2012. A conformational switch controls cell wall-remodelling enzymes required for bacterial cell division. Mol. Microbiol. **85:**768–781.
14. **Sham LT, Barendt SM, Kopecky KE, Winkler ME.** 2011. Essential PcsB putative peptidoglycan hydrolase interacts with the essential $FtsX_{Spn}$ cell division protein in *Streptococcus pneumoniae* D39. Proc. Natl. Acad. Sci. U. S. A. **108:**E1061–E1069.
15. **Yang DC, Peters NT, Parzych KR, Uehara T, Markovski M, Bernhardt TG.** 2011. An ATP-binding cassette transporter-like complex governs cell-wall hydrolysis at the bacterial cytokinetic ring. Proc. Natl. Acad. Sci. U. S. A. **108:**E1052–E1060.
16. **Crawford MA, Lowe DE, Fisher DJ, Stibitz S, Plaut RD, Beaber JW, Zemansky J, Mehrad B, Glomski IJ, Strieter RM, Hughes MA.** 2011. Identification of the bacterial protein FtsX as a unique target of chemokine-mediated antimicrobial activity against *Bacillus anthracis*. Proc. Natl. Acad. Sci. U. S. A. **108:**17159–17164.
17. **Garti-Levi S, Hazan R, Kain J, Fujita M, Ben-Yehuda S.** 2008. The FtsEX ABC transporter directs cellular differentiation in *Bacillus subtilis*. Mol. Microbiol. **69:**1018–1028.
18. **Schmidt KL, Peterson ND, Kustusch RJ, Wissel MC, Graham B, Phillips GJ, Weiss DS.** 2004. A predicted ABC transporter, FtsEX, is needed for cell division in *Escherichia coli*. J. Bacteriol. **186:**785–793.
19. **Arends SJ, Kustusch RJ, Weiss DS.** 2009. ATP-binding site lesions in FtsE impair cell division. J. Bacteriol. **191:**3772–3784.
20. **Reddy M.** 2007. Role of FtsEX in cell division of *Escherichia coli*: viability of ftsEX mutants is dependent on functional SufI or high osmotic strength. J. Bacteriol. **189:**98–108.
21. **Corbin BD, Wang Y, Beuria TK, Margolin W.** 2007. Interaction between cell division proteins FtsE and FtsZ. J. Bacteriol. **189:**3026–3035.
22. **Karimova G, Dautin N, Ladant D.** 2005. Interaction network among *Escherichia coli* membrane proteins involved in cell division as revealed by bacterial two-hybrid analysis. J. Bacteriol. **187:**2233–2243.
23. **Barendt SM, Land AD, Sham LT, Ng WL, Tsui HC, Arnold RJ, Winkler ME.** 2009. Influences of capsule on cell shape and chain formation of wild-type and *pcsB* mutants of serotype 2 *Streptococcus pneumoniae*. J. Bacteriol. **191:**3024–3040.
24. **Ng WL, Kazmierczak KM, Winkler ME.** 2004. Defective cell wall synthesis in *Streptococcus pneumoniae* R6 depleted for the essential PcsB putative murein hydrolase or the VicR (YycF) response regulator. Mol. Microbiol. **53:**1161–1175.
25. **Giefing-Kröll C, Jelencsics KE, Reipert S, Nagy E.** 2011. Absence of pneumococcal PcsB is associated with overexpression of LysM domain containing proteins. Microbiology **157:**1897–1909.
26. **de Leeuw E, Graham B, Phillips GJ, ten Hagen-Jongman CM, Oudega**

B, Luirink J. 1999. Molecular characterization of *Escherichia coli* FtsE and FtsX. Mol. Microbiol. **31:**983–993.
27. **Guiral S, Hénard V, Laaberki MH, Granadel C, Prudhomme M, Martin B, Claverys JP.** 2006. Construction and evaluation of a chromosomal expression platform (CEP) for ectopic, maltose-driven gene expression in *Streptococcus pneumoniae*. Microbiology **152:**343–349.
28. **Manson MD.** 2000. Allele-specific suppression as a tool to study protein-protein interactions in bacteria. Methods **20:**18–34.
29. **Mellroth P, Daniels R, Eberhardt A, Rönnlund D, Blom H, Widengren J, Normark S, Henriques-Normark B.** 2012. LytA, the major autolysin of *Streptococcus pneumoniae*, requires access to nascent peptidoglycan. J. Biol. Chem. **287:**11018–11029.
30. **Tomasz A, Waks S.** 1975. Mechanism of action of penicillin: triggering of the pneumococcal autolytic enzyme by inhibitors of cell wall synthesis. Proc. Natl. Acad. Sci. U. S. A. **72:**4162–4166.
31. **Peters NT, Dinh T, Bernhardt TG.** 2011. A fail-safe mechanism in the septal ring assembly pathway generated by the sequential recruitment of cell separation amidases and their activators. J. Bacteriol. **193:**4973–4983.
32. **García P, García JL, García E, Sánchez-Puelles JM, López R.** 1990. Modular organization of the lytic enzymes of *Streptococcus pneumoniae* and its bacteriophages. Gene **86:**81–88.
33. **Alvarez FJ, Orelle C, Davidson AL.** 2010. Functional reconstitution of an ABC transporter in nanodiscs for use in electron paramagnetic resonance spectroscopy. J. Am. Chem. Soc. **132:**9513–9515.
34. **Cui J, Davidson AL.** 2011. ABC solute importers in bacteria. Essays Biochem. **50:**85–99.
35. **Lanie JA, Ng WL, Kazmierczak KM, Andrzejewski TM, Davidsen TM, Wayne KJ, Tettelin H, Glass JI, Winkler ME.** 2007. Genome sequence of Avery's virulent serotype 2 strain D39 of *Streptococcus pneumoniae* and comparison with that of unencapsulated laboratory strain R6. J. Bacteriol. **189:**38–51.
36. **Ramos-Montañez S, Tsui HC, Wayne KJ, Morris JL, Peters LE, Zhang F, Kazmierczak KM, Sham LT, Winkler ME.** 2008. Polymorphism and regulation of the *spxB* (pyruvate oxidase) virulence factor gene by a CBS-HotDog domain protein (SpxR) in serotype 2 *Streptococcus pneumoniae*. Mol. Microbiol. **67:**729–746.
37. **Tsui HC, Mukherjee D, Ray VA, Sham LT, Feig AL, Winkler ME.** 2010. Identification and characterization of noncoding small RNAs in *Streptococcus pneumoniae* serotype 2 strain D39. J. Bacteriol. **192:**264–279.
38. **Sung CK, Li H, Claverys JP, Morrison DA.** 2001. An *rpsL* cassette, Janus, for gene replacement through negative selection in *Streptococcus pneumoniae*. Appl. Environ. Microbiol. **67:**5190–5196.
39. **Wayne KJ, Li S, Kazmierczak KM, Tsui HC, Winkler ME.** 2012. Involvement of WalK (VicK) phosphatase activity in setting WalR (VicR) response regulator phosphorylation level and limiting cross-talk in *Streptococcus pneumoniae* D39 cells. Mol. Microbiol. **86:**645–660.